Inorg. Chem. **2008**, *47*, 584–591

Tetra- and Dinuclear Nickel(II)–Vanadium(IV/V) Heterometal Complexes of a Phenol-Based N_2O_2 Ligand: Synthesis, Structures, and Magnetic and Redox Properties

Debdas Mandal,[†] Pabitra Baran Chatterjee,[†] Rakesh Ganguly,[†,⊥] Edward R. T. Tiekink,[‡] Rodolphe Clérac,[§] and Muktimoy Chaudhury*[,†]

Department of Inorganic Chemistry, Indian Association for the Cultivation of Science, Kolkata 700 032, India, Department of Chemistry, University of Texas, One UTSA Circle, San Antonio, Texas 78249-0698, and Université Bordeaux 1, CNRS, Centre de Recherche Paul Pascal UPR8641, 115 avenue du Dr. Albert Schweitzer, 33600 Pessac, France

Received September 28, 2007

The tetra- and binuclear heterometallic complexes of nickel(II)–vanadium(IV/V) combinations involving a phenol-based primary ligand, viz., *N*,*N*′-dimethyl-*N*,*N*′-bis(2-hydroxy-3,5-dimethylbenzyl)ethylenediamine (H_2L^1), are reported in this work. Carboxylates and β-diketonates have been used as ancillary ligands to obtain the tetranuclear complexes $[Ni^{II}_2V^{V}_2(RCOO)_2(L^1)_2O_4]$ (R = Ph, **1**; R = Me_3C, **2**) and the binuclear types [(β-diket)$Ni^{II}L^1V^{IV}O$(β-diket)] (**3** and **4**), respectively. X-ray crystallography shows that the tetranuclear complexes are constructed about an unprecedented heterometallic eight-membered $Ni_2V_2O_4$ core in which the $(L^1)^{2-}$ ligands are bound to the Ni center in a N_2O_2 mode and simultaneously bridge a V atom via the phenoxide O atoms. The *cis*-N_2O_4 coordination geometry for Ni is completed by an O atom derived from the bridging carboxylate ligand and an oxo O atom. The latter two atoms, along with a terminal oxide group, complete the O_5 square-pyramidal coordination geometry for V. Each of the dinuclear compounds, [(acac)$Ni^{II}L^1V^{IV}O$(acac)] (**3**) and [(dbm)$Ni^{II}L^1V^{IV}O$(dbm)] (**4**) [Hdbm = dibenzoylmethane], also features a tetradentate $(L^1)^{2-}$ ligand, Ni in an octahedral *cis*-N_2O_4 coordination geometry, and V in an O_5 square-pyramidal geometry. In **3** and **4**, the bridges between the Ni and V atoms are provided by the $(L^1)^{2-}$ ligand. The Ni···V separations in the structures lie in the narrow range of 2.9222(4) Å (**3**) to 2.9637(5) Å (**4**). The paramagnetic Ni centers ($S = 1$) in **1** and **2** are widely separated (Ni···Ni separations are 5.423 and 5.403 Å) by the double $V^{V}O_4$ bridge that leads to weak antiferromagnetic interactions ($J = -3.6$ and -3.9 cm^{-1}) and thus an $S_T = 0$ ground state for these systems. In **3** and **4**, the interactions between paramagnetic centers (Ni^{II} and V^{IV}) are also antiferromagnetic ($J = -8.9$ and -10.0 cm^{-1}), leading to an $S_T = {}^1/_2$ ground state. Compound **4** undergoes two one-electron redox processes at $E_{1/2} = +0.66$ and -1.34 V vs Ag/AgCl reference due to a $V^{IV/V}$ oxidation and a $Ni^{II/I}$ reduction, respectively, as indicated by cyclic and differential pulse voltammetry.

Introduction

The lithium−nickel vanadate system, $LiNiVO_4$, has been extensively studied in recent years because of its interesting properties.[1] More importantly, it is used as a cathode material in Li ion batteries, which are the contemporary choice as portable power sources for electronic and various other applications. These oxidic materials in the desired metastable structural forms are often difficult to synthesize, providing limited scope of their isolation. Recently, various organic/inorganic hybrid materials have been used as structure-directing precursor components to facilitate these syntheses.[2]

* To whom correspondence should be addressed. E-mail: icmc@iacs.res.in.
[†] Indian Association for the Cultivation of Science.
[⊥] Present address: Department of Chemistry, National University of Singapore, Singapore 117543, Singapore.
[‡] University of Texas.
[§] Université Bordeaux 1, CNRS, Centre de Recherche Paul Pascal.

(1) (a) Reddy, M. V.; Pecquenard, B.; Vinatier, P.; Levasseur, A. *J. Phys. Chem. B* **2006**, *110*, 4301. (b) Lu, C.-H.; Liou, S.-J. *J. Mater. Sci. Lett.* **1998**, *17*, 733. (c) Zhao, Z.; Ma, J.; Xie, L.; Tian, H.; Zhou, J.; Hu, Y.; Huang, X.; Wu, P.; Dai, J.; Zhee, Z.; Wang, H.; Chen, H. *J. Am. Ceram. Soc.* **2005**, *88*, 2622.
(2) Chestnut, D. J.; Hagrman, D.; Zapf, P. J.; Hammond, R. P.; LaDuca, R., Jr.; Haushalter, R. C.; Zubieta, J. *Coord. Chem. Rev.* **1999**, *190*−*192*, 737.

10.1021/ic701925j CCC: $40.75
Published on Web 12/28/2007

A few such hybrid compounds with nickel(II)−vanadium(IV/V) combinations, prepared mostly by hydrothermal synthesis, have been reported thus far.[3−10] These compounds have extended structures, some of these are really fascinating. There are also a few reports involving discrete nickel(II)−vanadium(IV/V) compounds.[11−14]

Herein, we report two sets of discrete heterometallic compounds with nickel(II)−vanadium(IV/V) combinations using a phenol-based tetradentate N_2O_2 ligand (H_2L^1) as the primary metal chelator. In the tetranuclear types of compounds $[Ni_2V_2(RCOO)_2(L^1)_2O_4]$ (**1** and **2**), carboxylates are used as ancillary bridging ligands to bind the Ni^{II} and $V^{V}O$ centers, while in the dinuclear compounds [(β-diket)NiL^1-VO(β-diket)] (**3** and **4**), β-diketonates are the preferred choice as ancillary ligands. X-ray crystallography, electronic spectroscopy, and magnetic susceptibility measurements at variable temperatures have been carried out to characterize these compounds. Redox properties of the dinuclear compounds (**3** and **4**) have also been investigated by cyclic and differential pulse voltammetry as well as by constant potential coulometry.

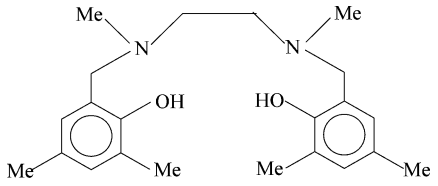

H_2L^1

Experimental Section

Materials. The precursor complexes $[VO(acac)_2]$,[15] $[VO(dbm)_2]$,[16] and $[(n\text{-}C_4H_9)_4N]_3[H_3V_{10}O_{28}]$[17] were prepared following reported methods. $[Ni(H_2L^1)(PhCOO)_2]$, $[Ni(H_2L^1)(Me_3CCOO)_2]$, and $[NiL^1(H_2O)_2]\cdot 0.5H_2O$ were prepared as described elsewhere.[18] Dibenzoylmethane (Hdbm) was purchased from Aldrich. All other reagents were commercially available and used as received. Solvents were of analytical grade, were dried from appropriate reagents, and were distilled under nitrogen prior to their use.[19]

Preparation of Complexes. $[Ni_2V_2(PhCOO)_2(L^1)_2O_4]$ (1). $[Ni(H_2L^1)(PhCOO)_2]$ (0.065 g, 0.1 mmol) in acetone (10 mL) was mixed with a solution of $[(n\text{-}C_4H_9)_4N]_3[H_3V_{10}O_{28}]$ (0.17 g, 0.1 mmol) in 10 mL of acetonitrile. The resulting solution was kept in the open air for slow evaporation. After 1 day, a red crystalline compound was obtained along with some X-ray-diffraction-quality crystals. Yield: 0.05 g (30%). Anal. Calcd for $C_{58}H_{70}N_4O_{12}Ni_2V_2$: C, 56.38; H, 5.67; N, 4.53. Found: C, 56.44; H, 5.95; N, 4.36. IR (KBr disk, cm^{-1}): 3439, 2911, 1591, 1545, 1475, 1374, 1316, 1255, 1226, 954, 868, 816, 720, 512. $\mu = 4.2\ \mu_B$ at 25 °C.

$[Ni_2V_2(Me_3CCOO)_2(L^1)_2O_4]$ (2). This compound was prepared in the same manner as that described above for **1** using $[Ni(H_2L^1)(Me_3CCOO)_2]$ as the precursor nickel(II) compound. Yield: 25%. Anal. Calcd for $C_{54}H_{78}N_4O_{12}Ni_2V_2$: C, 54.24; H, 6.53; N, 4.69. Found: C, 54.22; H, 6.27; N, 4.65. IR (KBr disk, cm^{-1}): 3434, 2920, 1551, 1476, 1400, 1358, 1317, 1230, 960, 864, 812, 512. $\mu = 4.1\ \mu_B$ at 25 °C.

$[(acac)NiL^1VO(acac)]$ (3). $[NiL^1(H_2O)_2]\cdot 0.5H_2O$ (0.23 g, 0.5 mmol) was taken in 30 mL of acetonitrile. $[VO(acac)_2]$ (0.13 g, 0.5 mmol) in solids was added to this solution. The mixture was refluxed for ca. 2 h, at which time a green solution was obtained. The solution was cooled and rotary evaporated to about 10 mL volume. The solution was kept in the open air for an overnight period, after which a green crystalline compound along with some diffraction-grade crystals were obtained. Yield: 0.15 g (44%). Anal. Calcd for $C_{32}H_{44}N_2O_7NiV$: C, 56.61; H, 6.48; N, 4.13. Found: C, 56.81; H, 6.54; N, 4.34. IR (KBr disk, cm^{-1}): 3459, 2917, 1593, 1518, 1474, 1394, 1247, 981, 923, 813, 783, 459. UV−vis (CH_2Cl_2) [λ_{max}/nm (ϵ/mol^{-1} cm^2)]: 857 (75), 631 (50), 448 (sh), 307 (20 000), 231 (21 100). ESI-MS in CH_2Cl_2: *m*/*z* 677 ($M + H^+$). $\mu = 3.5\ \mu_B$ at 25 °C.

$[(dbm)NiL^1VO(dbm)]\cdot CH_3CN$ (4). A mixture of $[NiL^1(H_2O)_2]\cdot 0.5H_2O$ (0.23 g, 0.5 mmol) and $[VO(dbm)_2]$ (0.25 g, 0.5 mmol) in acetonitrile (30 mL) was allowed to reflux for 1 h, affording a yellowish-green solution that was concentrated by rotary evaporation to ca. 10 mL volume and filtered. The filtrate upon standing overnight in a refrigerator (4 °C) yielded a dark crystalline compound along with some X-ray-diffraction-quality crystals. The compound was collected by filtration, washed with diethyl ether (2 × 5 mL), and dried in vacuo. Yield: 0.25 g (54%). Anal. Calcd for $C_{54}H_{55}N_3O_7NiV$: C, 66.96; H, 5.68; N, 4.34. Found: C, 66.63; H, 5.30; N, 4.19. IR (KBr disk, cm^{-1}): 3433, 2912, 1596, 1548, 1521, 1473, 1398, 1365, 1309, 1245, 987, 811, 754, 632, 570, 368. UV−vis (CH_2Cl_2) [λ_{max}/nm (ϵ/mol^{-1} cm^2)]: 874 (75), 649 (45), 503 (90), 371 (31 000), 255 (36 000) 226 (32 000). ESI-MS in CH_2Cl_2: *m*/*z* 926 ($M - CH_3CN + H^+$). $\mu = 3.4\ \mu_B$ at 25 °C.

Physical Measurements. IR spectroscopic measurements were done on samples pressed into KBr disks using a Nicolet 520 FTIR spectrometer. Electrospray ionization mass spectrometry (ESI-MS) spectra (in positive ion mode) were recorded on a QTOF model YA263 micromass spectrometer. Electronic spectra in solution were recorded on a Perkin-Elmer Lambda 950 UV/vis/NIR spectrophotometer. Elemental analyses (for C, H, and N) were performed in this laboratory (at IACS) using a Perkin-Elmer model 2400 analyzer.

Magnetic susceptibility and magnetization experiments on powdered polycrystalline samples were performed in the temperature range 1.8−300 K on a Quantum Design SQUID MPMS-XL magnetometer. The samples of **1**−**4** were packed in a sealed plastic

(3) Xiao, D.; Hou, Y.; Wang, E.; Lu, J.; Li, Y.; Xu, L.; Hu, C. *Inorg. Chem. Commun.* **2004**, *7*, 437.
(4) Liu, C.-M.; Hou, Y.-L.; Zhang, J.; Gao, S. *Inorg. Chem.* **2002**, *41*, 140.
(5) Dai, Z.; Chen, X.; Shi, Z.; Zhang, D.; Li, G.; Feng, S. *Inorg. Chem.* **2003**, *42*, 908.
(6) Xiao, D.; Li, Y.; Wang, E.; Wang, S.; Hou, Y.; De, G.; Hu, C. *Inorg. Chem.* **2003**, *42*, 7652.
(7) Liu, C.-M.; Luo, J.-L.; Zhang, D.-Q.; Wang, N.-L.; Chen, Z.-J.; Zhu, D.-B. *Eur. J. Inorg. Chem.* **2004**, 4774.
(8) Liu, C.-M.; Gao, S.; Hu, H.-M.; Jin, X.; Kou, H.-Z. *J. Chem. Soc., Dalton Trans.* **2002**, 598.
(9) Shi, Z.; Feng, S.; Gao, S.; Zhang, L.; Yang, G.; Hua, J. *Angew. Chem., Int. Ed.* **2000**, *39*, 2325.
(10) LaDuca, R. L., Jr.; Rarig, R. S., Jr.; Zubieta, J. *Inorg. Chem.* **2001**, *40*, 607.
(11) Glick, M. D.; Lintvedt, R. L.; Gavel, D. P.; Tomlonovic, B. *Inorg. Chem.* **1976**, *15*, 1654.
(12) Rauchfuss, T. B.; Gammon, S. D.; Weatherill, T. D.; Wilson, S. R. *New J. Chem.* **1988**, *12*, 373.
(13) Nanda, K. K.; Mohanta, S.; Ghosh, S.; Mukherjee, M.; Helliwell, M.; Nag, K. *Inorg. Chem.* **1995**, *34*, 2861.
(14) Do, J.; Jacobson, A. J. *Inorg. Chem.* **2001**, *40*, 2468.
(15) Rowe, R. A.; Jones, M. M. *Inorg. Synth.* **1957**, *5*, 113.
(16) Ikeda, S.; Yamamoto, A.; Kurita, S.; Takahashi, K.; Watanabe, T. *Inorg. Chem.* **1966**, *5*, 611.
(17) Day, V. W.; Klemperer, W. G.; Maltbie, D. J. *J. Am. Chem. Soc.* **1987**, *109*, 2991.
(18) Mandal, D. Ph.D. Thesis, Jadavpur University, Kolkata, India, 2007.
(19) Perrin, D. D.; Armarego, W. L. F.; Perrin, D. R. *Purification of Laboratory Chemicals*, 2nd ed.; Pergamon: Oxford, U.K., 1980.

Table 1. Crystallographic Parameters and Refinement Details for **1**−**4**

parameter	**1**	**2**	**3**	**4**
formula	$C_{58}H_{70}N_4Ni_2O_{12}V_2$	$C_{54}H_{78}N_4Ni_2O_{12}V_2$	$C_{32}H_{44}N_2NiO_7V$	$C_{52}H_{52}N_2NiO_7V{\cdot}C_2H_3N$
fw	1234.44	1194.50	678.32	967.66
cryst syst	orthorhombic	monoclinic	monoclinic	triclinic
space group	*Pbca*	$P2_1/c$	$P2_1/c$	$P\bar{1}$
a, Å	13.3548(6)	12.0770(7)	11.9355(15)	11.2938(4)
b, Å	17.9752(7)	17.4402(10)	18.902(2)	12.8014(5)
c, Å	23.1855(10)	13.4539(8)	14.8328(18)	17.2832(7)
α, deg	90	90	90	83.331(1)
β, deg	90	97.988(1)	96.672(3)	86.659(1)
γ, deg	90	90	90	77.124(1)
V, Å^3	5565.8(4)	2806.2(3)	3323.8(7)	2418.08(16)
Z	4	2	4	2
μ, cm^{-1}	1.058	1.046	0.894	0.638
D_x, g cm^{-3}	1.473	1.414	1.356	1.329
no. of reflns	44 603	23 632	27 479	20 669
no. of unique reflns	8127	7939	9687	13 282
no of obs reflns with $I > 2\sigma(I)$	6190	6313	7343	10 655
R (obs data)	0.069	0.042	0.040	0.044
a, *b* in the weighting scheme	0.062, 6.326	0.062, 0.428	0.057, 0	0.064, 0.394
R_w (all data)	0.162	0.111	0.106	0.120
CCDC no.	660946	660947	660948	660949

bag. The raw data were corrected for the sample holder and the orbital diamagnetic contributions calculated from Pascal's constant.[20] The samples have been checked for ferromagnetic impurities that were found to be systematically absent by measuring the field dependence of magnetization at $T = 100$ K.

Electrochemical measurements were performed at room temperature in an electrochemical cell (15 mL capacity) fitted with a platinum working electrode, a platinum wire counter electrode, and an inert-gas inlet. All potentials were measured against an Ag/AgCl (3 M NaCl solution) reference electrode. Dry degassed acetonitrile containing 0.1 M tetrabutylammonium perchlorate (TBAP) as the background electrolyte was used during the measurements. Bulk electrolyses were performed with the use of a platinum gauze working electrode. The apparatus was a PAR model 273A scanning potentiostat. The ferrocenium/ferrocene couple was used as the internal standard.

X-ray Crystallography. Intensity data were measured at 223(2) K for red **1**, red-brown **2**, green **3**, and green-yellow **4**, characterized as an acetonitrile solvate, on a Bruker SMART CCD employing Mo Kα radiation so that θ_{max} was 30° (30.1° for **2**). Data processing and empirical absorption correction were accomplished with the programs *SAINT*[21] and *SADABS*,[22] respectively. The structures were solved by heavy-atom methods,[23] and refinement (anisotropic displacement parameters, hydrogen atoms in the riding model approximation, and a weighting scheme of the form $w = 1/[\sigma^2(F_o^2) + aP^2 + bP]$ for $P = (F_o^2 + 2F_c^2)/3$) was on F^2.[24] In the refinement of **2**, two positions were resolved for the methyl groups of the *tert*-butyl residue, and from refinement, the site occupancy factors for the components were determined as 0.571(11) and 0.429(11), respectively; the component atoms were refined anisotropically. In each refinement, the maximum residual electron density peak was less than 1 e Å^{-3}. Crystallographic data and final refinement details are given in Table 1. Figures 1a, 2a, and S2 and S3 (in the Supporting Information) were drawn with *ORTEP*[25] at the 50% probability level, and Figures 1b and 2b were drawn with the *DIAMOND* program with arbitrary spheres.[26] Data manipulation and analysis was with *teXsan*.[27]

Results and Discussion

Syntheses. The synthetic strategy adopted in this work is outlined in Scheme 1. The tetranuclear complexes **1** and **2** have been synthesized simply by mixing decavanadate $[(n\text{-}C_4H_9)_4N]_3[H_3V_{10}O_{28}]$ with stoichiometric amounts (1:1 mole ratio) of carboxylate-based precursor compounds $[Ni(H_2L^1)(RCOO)_2]$ (R = Ph or Me_3C) in an acetone/acetonitrile (1:1, v/v) solvent mixture. The procedure for the synthesis of the binuclear compounds **3** and **4** is also quite straightforward and involves mixing of $[NiL^1(H_2O)_2]{\cdot}0.5H_2O$ with the corresponding $[VO(\beta\text{-diket})_2]$ in a 1:1 mole ratio in acetonitrile. Both compounds **1** and **2** are sparingly soluble in common organic solvents.

IR spectra of the complexes **1**−**4** display all of the characteristic bands of the coordinated $(L^1)^{2-}$ ligand. One such prominent band appears in the region 1255−1230 cm^{-1} due to ν(C−O/phenolate) stretching vibrations. Of particular interest in the spectra of **1** and **2** is the appearance of a strong band at ca. 1550 cm^{-1} due to ν_{asym}(COO) vibrations of the ancillary carboxylate ligand. Corresponding signature vibrations for the *β*-diketonate moiety in **3** and **4** appear in the form of a twin band at ca. 1595 and 1520 cm^{-1} due to ν(C═C) and ν(C═O) stretching bands, respectively.[28] A single sharp band in the 990−960 cm^{-1} region is also observed in these compounds due to V═O$_t$ terminal stretches. In addition, **1** and **2** show a moderately sharp band at ca. 815 cm^{-1} possibly due to V−O−Ni bridge vibrations.

(20) *Theory and Applications of Molecular Paramagnetism*; Boudreaux, E. A., Mulay, L. N., Eds.; John Wiley & Sons: New York, 1976.
(21) *SAINT*, version 5.6; Bruker AXS Inc.: Madison, WI, 2000.
(22) (a) Sheldrick, G. M. *SADABS*; University of Göttingen: Göttingen, Germany, 2000. (b) Blessing, R. *SADABS*. *Acta Crystallogr.* **1995**, *A51*, 33.
(23) Beurskens, P. T.; Admiraal, G.; Beurskens, G.; Bosman, W. P.; García-Granda, S.; Smits, J. M. M.; Smykalla, C. *The DIRDIF program system*; Technical Report; Crystallography Laboratory, University of Nijmegen: Nijmegen, The Netherlands, 1992.
(24) Sheldrick, G. M. *SHELXL97: Program for crystal structure refinement*; University of Göttingen: Göttingen, Germany, 1997.
(25) Johnson, C. K. *ORTEP*; Report ORNL-5138; Oak Ridge National Laboratory: Oak Ridge, TN, 1976.
(26) *DIAMOND, Visual Crystal Structure Information System*, version 2.1e; Bonn, Germany 2002.
(27) *teXsan: Structure Analysis Software*; Molecular Structure Corp.: The Woodlands, TX, 1997.
(28) Nakamoto, K. *Infrared and Raman Spectra of Inorganic and Coordination Compounds*, 3rd ed.; Wiley-Interscience: New York, 1978.

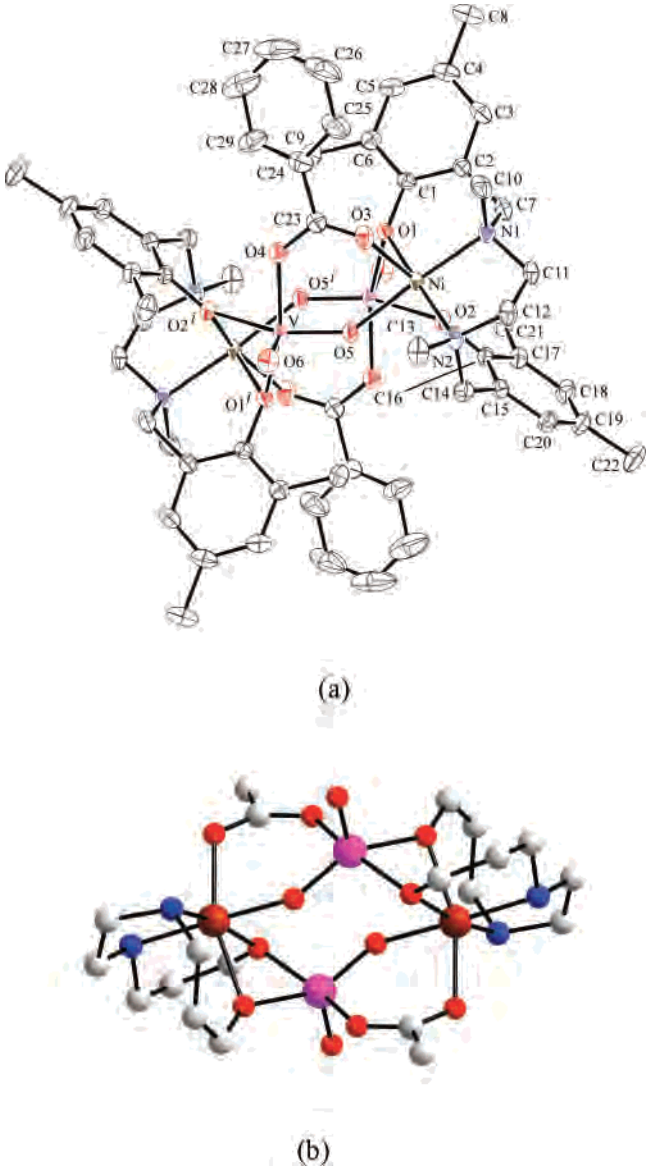

Figure 1. (a) Molecular structure and crystallographic numbering scheme for **1**. The dinuclear molecule is disposed about a crystallographic center of inversion. Symmetry operation *i*: $1 - x, -y, 1 - z$. Hydrogen atoms have been omitted for clarity. (b) Molecular core in **1**. Color code: Ni, brown; V, pink; O, red; N, blue; C, gray. Hydrogen atoms are omitted.

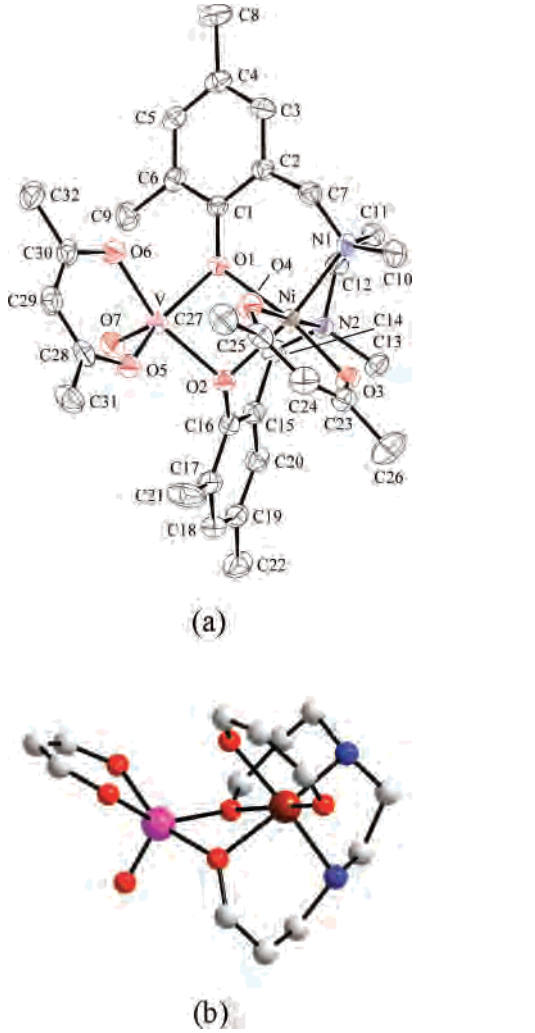

Figure 2. (a) Molecular structure and crystallographic numbering scheme for **3**. Hydrogen atoms have been omitted for clarity. (b) Core structure for **3**. Color code: same as that for Figure 1b.

Mass Spectroscopy. The ESI-MS spectrum (in positive ion mode) of **3** in an acetonitrile medium displays the molecular ion peak at *m*/*z* 677 ($M + H^+$) with 100% relative abundance and the expected isotope pattern. Likewise, **4** also shows the molecular ion peak at *m*/*z* 926 ($M - CH_3CN + H^+$, 100% relative abundance). The isotope distribution pattern for the base peak of **3** is displayed in Figure S1 (Supporting Information) as a representative example, together with its simulation pattern. The results confirm the presence of these binuclear compounds with the desired heterometal combination, devoid of any metal-ion scrambling. The lack of solubilities of the tetranuclear compounds **1** and **2** in common organic solvents has prevented us from measuring the ESI-MS spectra of these compounds.

Description of Crystal Structures. The tetranuclear compounds **1** and **2** are isostructural. The representative ORTEP structure for **1** is shown in Figure 1a and that of **2** in Figure S2 in the Supporting Information. Identical atom-labeling schemes have been adopted for both structures for easy comparison of their relevant metrical parameters (Table 2). Compound **1** crystallizes in the orthorhombic space group *Pbca* with four molecules per unit cell, while **2** has the monoclinic space group $P2_1/c$ with two molecules accommodated in the unit cell. The molecules have centrosymmetric structures, with each half containing a dinuclear [Ni−VO(μ-O)L^1(μ-RCOO)] core. The Ni^{II} center in this core has a distorted octahedral geometry, completed by the O(1), N(1), N(2), and O(2) donor atoms, all coming from the ligand $(L^1)^{2-}$, together with O(5) and O(3) atoms, contributed by the μ-oxo and μ-carboxylato moieties, respectively. The phenoxo oxygen atoms O(1) and O(2) along with N(2) and the carboxylato oxygen O(3) form the NO_3 basal plane, while the apical positions are taken up by the remaining amino nitrogen N(1) and the bridging oxo ligand O(5). The trans angles O(1)−Ni−N(2) [169.28(10)°] and O(5)−Ni−N(1) [176.65(11)°] in **1** are close to linearity, while the third one, O(3)−Ni−O(2) [158.83(10)°], is slightly off because of restrictions imposed by the two bridging atoms O(3) and O(2). Corresponding angles in **2** are 168.56(6)°, 174.88(6)°,

Scheme 1 [a]

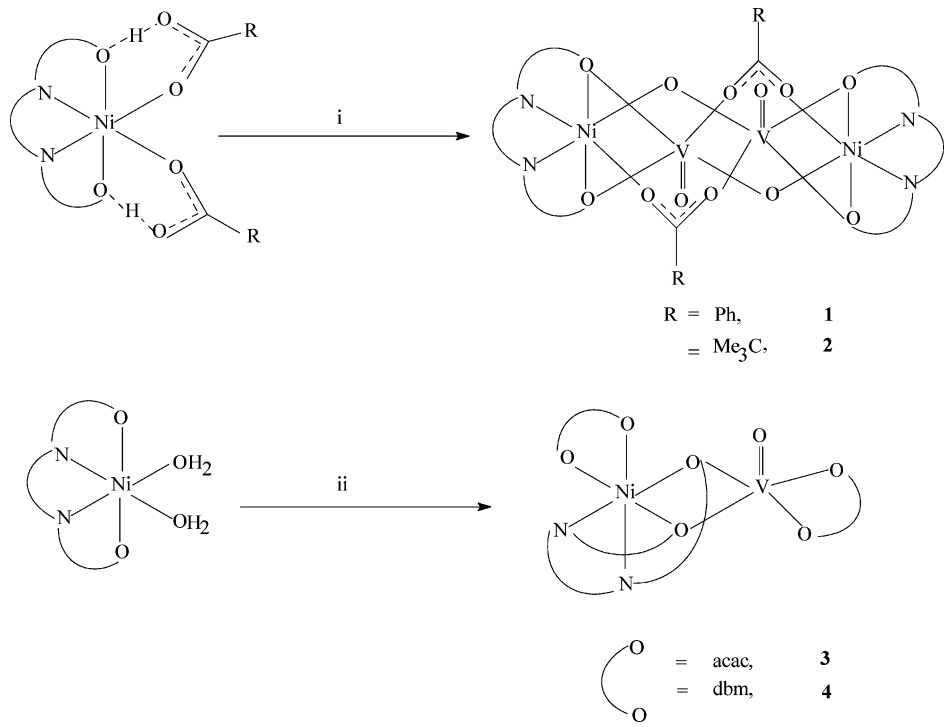

[a] Conditions: (i) $[(n\text{-}C_4H_9)_4N]_3[H_3V_{10}O_{28}]$, in an acetonitrile/acetone mixture. (ii) $[VO(\beta\text{-diket})_2]$, in acetonitrile under reflux.

Table 2. Selected Bond Distances (Å) and Angles (deg) for **1** and **2**

	1	**2**
	Bond Distances (Å)	
Ni−O1	2.062(2)	2.0481(12)
Ni−O2	2.072(2)	2.0802(13)
Ni−O3	2.088(2)	2.0475(14)
Ni−O5	2.014(2)	2.0213(13)
Ni−N1	2.066(3)	2.0808(17)
Ni−N2	2.071(3)	2.0657(16)
V−O4	1.992(2)	1.9867(14)
V−O5	1.665(2)	1.6637(14)
V−O6	1.597(2)	1.5994(14)
V−O1^i	1.970(2)[a]	1.9873(13)[b]
V−O2^i	2.044(2)[a]	2.0463(13)[b]
Ni···V^i	2.9227(7)[a]	2.9257(4)[b]
	Bond Angles (deg)	
O5−Ni−O3	85.05(10)	86.59(6)
O5−Ni−N1	176.65(11)	174.88(6)
N1−Ni−N2	85.68(11)	85.43(6)
O1−Ni−O2	74.68(9)	74.71(5)
O1−Ni−N2	169.28(10)	168.56(6)
O3−Ni−O2	158.83(10)	160.57(5)
O5−V−O2^i	143.57(11)[a]	143.55(6)[b]
O4−V−O1^i	156.43(10)[a]	158.60(5)[b]

[a] Symmetry operation i: $1 - x, -y, 1 - z$. [b] Symmetry operation i: $-x, -y, -z$.

and 160.57(5)°, respectively. In **2**, the cis angles at Ni in the equatorial plane range between 101.98(6)° and 74.71(5)°, totaling 360.11°. The corresponding angles in **1** are in the range between 102.23(11)° and 74.68(9)°. The average Ni−O and Ni−N distances are 2.0541 and 2.0708 Å, respectively, which are as expected for a high-spin octahedral Ni^{II} compound.[29] The V centers exist in a distorted square-pyramidal geometry ($\tau = 0.25$ and 0.24),[30] with four basal positions being taken up by O(2) and O(1) belonging to the bridging phenoxo moiety of the ligand $(L^1)^{2-}$, together with O(5) and O(4), contributed by the μ-oxo and μ-carboxylato groups, respectively. The axial site is occupied by the oxo ligand O(6), which forms angles in the range 98.49(12)−110.84(11)° [96.46(7)−110.65(7)° for **2**] with the basal plane. The trans angles in the basal plane O(5)−V−O(2) and O(4)−V−O(1) are 143.57(11)° [143.55(6)°] and 156.43(10)° [158.60(5)°], respectively, which force the vanadium atom out of the basal plane by 0.425 Å (0.408 Å) toward the apical oxygen O(6) atom. The terminal V−O(6) distance 1.597(2) Å [1.5994(14) Å] is in the expected range, while the bridging V−O(5) distance 1.6637(14) Å [1.665(2) Å] is shorter than what is normally observed.[31] The Ni···V separation is 2.9227(7) Å [2.9257(4) Å], and the Ni−O−V bridge angle is 141.01(14)° [139.80(8)°]. Also in these tetranuclear compounds, the Ni···Ni and V···V separations are 5.4233(6) Å [5.4033(4) Å] and 3.4301(8) Å [3.4501(4) Å], respectively. Thus, the distant Ni centers in these molecules are connected together by V^VO_4 tetrahedra formed by a pair of μ-oxo and μ-carboxylato bridges. The molecular core in **1** is displayed in Figure 1b, which highlights the coordination modes of the constituent ligands and the presence of the centrosymmetric heterometallic eight-membered $Ni_2V_2O_4$ ring, stabilized by alternating oxo and phenoxide O bridges.

The nickel(II)−oxovanadium(IV) heterodinuclear complexes **3** and **4** have essentially similar structures (displayed

(29) (a) Berti, E.; Caneschi, A.; Daiguebonne, C.; Dapporto, P.; Formica, M.; Fusi, V.; Giorgi, L.; Guerri, A.; Micheloni, M.; Paoli, P.; Pontellini, R.; Rossi, P. *Inorg. Chem.* **2003**, *42*, 348. (b) Shimazaki, Y.; Huth, S.; Karasawa, S.; Hirota, S.; Naruta, Y.; Yamauchi, O. *Inorg. Chem.* **2004**, *43*, 7816.

(30) Addition, A. W.; Rao, T. N.; Reedijk, J.; van Rijn, J.; Verschoor, G. C. J. *J. Chem. Soc., Dalton Trans.* **1984**, 1349.

(31) (a) Dutta, S. K.; Kumar, S. B.; Bhattacharya, S.; Tiekink, E. R. T.; Chaudhury, M. *Inorg. Chem.* **1997**, *36*, 4954. (b) Dutta, S. K.; Samanta, S.; Kumar, S. B.; Han, O. H.; Burckel, P.; Pinkerton, A. A.; Chaudhury, M. *Inorg. Chem.* **1999**, *38*, 1982.

Table 3. Selected Bond Distances (Å) and Angles (deg) for **3** and **4**

	3	**4**
	Bond Distances (Å)	
Ni−O1	2.1257(12)	2.1035(11)
Ni−O2	2.0283(12)	2.0281(12)
Ni−O3	2.0098(13)	2.0094(12)
Ni−O4	2.0148(12)	2.0176(12)
Ni−N1	2.0851(15)	2.0836(16)
Ni−N2	2.0879(14)	2.0771(14)
V−O1	1.9864(12)	1.9926(12)
V−O2	2.0013(12)	2.0085(11)
V−O5	1.9857(13)	1.9866(12)
V−O6	1.9849(13)	1.9609(12)
V−O7	1.5907(13)	1.5885(14)
Ni···V	2.9637(5)	2.9222(4)
	Bond Angles (deg)	
O3−Ni−O4	92.09(5)	90.93(5)
O3−Ni−O1	169.72(5)	168.26(5)
O1−Ni−O2	77.78(5)	77.50(5)
O2−Ni−N1	169.02(5)	169.09(5)
O4−Ni−N2	172.44(5)	173.88(5)
N1−Ni−N2	84.96(6)	86.26(6)
O1−V−O2	81.73(5)	80.56(5)
V−O2−Ni	94.69(5)	92.76(5)
V−O1−Ni	92.17(5)	90.98(5)

in Figures 2a and S3 in the Supporting Information, respectively) with almost identical metrical parameters (Table 3). Complex **3** crystallizes in the monoclinic space group $P2_1/c$, while **4** has the triclinic space group $P\bar{1}$, with four and two molecules in their respective unit cells. The Ni^{II} sites in these molecules have distorted octahedral geometry, comprised of O(1), N(1), N(2), and O(2) donor sites provided by the tetradentate $(L^1)^{2-}$ ligand, together with O(3) and O(4) donor atoms from the β-diketonate moiety. The basal plane is comprised of O(1), N(1), O(3), and O(2) atoms, while the apical positions are taken up by N(2) and O(4). The nickel atoms are displaced marginally (by 0.042 and 0.061 Å for **3** and **4**, respectively) from these least-squares basal planes toward the apical oxo atom O(4). In **3**, the trans angles O(4)−Ni−N(2) [172.44(5)°], O(2)−Ni−N(1) [169.02(5)°], and O(3)−Ni−O(1) [169.72(5)°] are slightly short of linearity. Corresponding angles in **4** are 173.88(5)°, 169.09(5)°, and 168.26(5)°, respectively. The average Ni−O [2.0446 Å (2.0396 Å for **4**)] and Ni−N [2.0865 Å (2.0803 Å)] distances are also in the range, expected for a high-spin Ni^{II} compound.[29] The V^{IV} sites have square-pyramidal geometry (τ = 0.24), with basal positions being occupied by O(5) and O(6) atoms coming from a β-diketonate moiety, together with the bridging donors O(1) and O(2), both contributed by phenoxo oxygen atoms from $(L^1)^{2-}$. The trans angles O(2)−V−O(6) {159.91(5)° [155.21(6)° for **4**]} and O(1)−V−O(5) {145.73(5)° [149.14(5)°]} are somewhat compressed, giving evidence that the V center is shifted appreciably (by ca. 0.46 Å) from the least-squares basal plane toward the apical oxo atom O(7). The terminal V−O(7) distance {1.5907(13) Å [1.5885(14) Å]} is as expected,[31] and the cis angles that it makes with the equatorial plane are in the range 99.46(6)−111.27(6)° [100.57(6)−110.28(6)°]. The Ni···V separation is 2.9637(5) Å [2.9222(4) Å], and the metal centers are connected by a pair of phenoxo bridges. The core molecular structure of **3** is shown in Figure 2b and is repeated in the

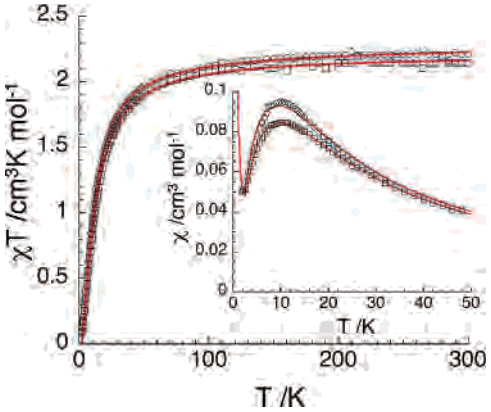

Figure 3. Temperature dependence of the χT product for **1** (○, opened circles) and **2** (□, opened squares) at H = 0.1 T. Inset: Temperature dependence of the magnetic susceptibility for **1** (○, opened circles) and **2** (□, opened squares) at H = 0.1 T. The solid lines are the best fits of the data using the Heisenberg S = 1 dimer model described in the text.

structure of **4**. Thus, the ancillary β-diketonate ligands have only a limited influence in controlling the overall structures of **3** and **4**.

Magnetic Properties. Magnetic susceptibility measurements for the polycrystalline samples of the complexes **1**−**4** have been carried out in the temperature range 1.8−300 K. For the tetranuclear complexes **1** and **2**, the χT vs T and χ vs T plots displayed in Figure 3 show that they exhibit almost the same magnetic behavior. These measurements suggest that the Ni^{II} (S = 1) centers in **1** and **2** are antiferromagnetically coupled through the diamagnetic oxovanadium(V) moiety because the χT product gradually decreases from 2.22 and 2.14 cm^3 K mol^{-1} for **1** and **2**, respectively (300 K), to 0.09 cm^3 K mol^{-1} at 1.82 K for both compounds. On the basis of the structure consisting of two paramagnetic centers in these complexes, the magnetic data have been modeled using an isotropic Heisenberg model in the weak-field approximation. Thus, the theoretical susceptibility has been deduced from the van Vleck equation[32] considering the following Hamiltonian: $H = -2J(S_1 \cdot S_2)$, where J is the isotropic exchange interaction between Ni^{II} sites and S_i is the spin operator for each metal center (S_i = 1 Ni^{II} with i = 1−2).[33] In order to reproduce the low-temperature magnetic susceptibility typically below 10 K, an additional paramagnetic contribution (S = 1 Curie law) has been taken into account in the fitting procedure, as shown in eq 1.

$$\chi = (1-\rho)\frac{2Ng^2\mu_B{}^2}{k_BT}\frac{\exp(2J/k_BT)+5\exp(6J/k_BT)}{1+3\exp(2J/k_BT)+5\exp(6J/k_BT)} + \rho\frac{2Ng^2\mu_B{}^2}{3k_BT} \quad (1)$$

As shown in Figure 3 by the solid lines, the experimental data are well reproduced by this approach and the best sets of parameters obtained are $J = -3.6(1)$ cm^{-1}, g = 2.20(2), and ρ = 0.067 for **1** and $J = -3.9(1)$ cm^{-1}, g = 2.16(2), and ρ = 0.074 for **2**. The negative sign of these magnetic

(32) van Vleck, J. H. *The Theory of Electric and Magnetic Susceptibility*; Oxford University Press: Oxford, U.K., 1932.
(33) Kambe, K. *J. Phys. Soc. Jpn.* **1950**, *5*, 48.

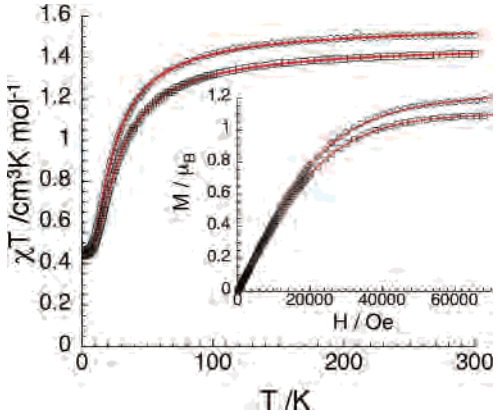

Figure 4. Temperature dependence of the χT product for **3** (○, opened circles) and **4** (□, opened squares) at $H = 0.1$ T. The solid lines are the best fits of the data using the Heisenberg $S = {}^1/_2$ and 1 dimer model described in the text. Inset: Field dependence of the magnetization at 1.8 K for **3** (○, opened circles) and **4** (□, opened squares). The solid lines are the best fits of the data using the $S = {}^1/_2$ Brillouin functions.

interactions implies an $S_T = 0$ spin ground state for these complexes. The low values of the ρ parameters confirm the presence of a weak amount of paramagnetic impurities in these compounds. It is worth noting that such an impurity is almost always observed in a compound with a diamagnetic ground state because this extrinsic contribution becomes the only observable at low temperatures. Of particular interest here are the two widely separated Ni^{II} centers (Ni···Ni separations, 5.4233(6) and 5.4033(4) Å for **1** and **2**, respectively) linked by a O−V−O bridge that provides a relatively efficient pathway for antiferromagnetic coupling. Liu et al.[34] have reported a nickel(II)−vanadium(V) compound with an extended molecular structure in which the octahedral Ni^{II} centers are connected by diamagnetic $[V_2O_6]^{2-}$ linkers, providing a Ni···Ni separation of 5.413 Å. This compound $[Ni(bipy)(H_2O)V_2O_6]_\alpha$ also revealed antiferromagnetic exchange interactions between the participating Ni^{II} centers as observed in **1** and **2**.

For the nickel(II)−vanadium(IV) dinuclear complexes **3** and **4**, the χT vs T plots are shown in Figure 4. For both compounds, the χT product exhibits a sharp decrease from 1.52 and 1.42 cm^3 K mol^{-1} (300 K) to 0.45 and 0.43 cm^3 K mol^{-1} at 1.82 K for **3** and **4**, respectively, indicating intracomplex antiferromagnetic interactions. The magnetic data have been modeled using an isotropic Heisenberg model [with the following spin Hamiltonian: $H = -2J(S_{Ni}\cdot S_V)$] in the weak-field approximation considering an isotropic exchange between $S_{Ni} = 1$ Ni^{II} and $S_V = {}^1/_2$ V^{IV} metal ions. The theoretical susceptibility[35,36] has been deduced from the van Vleck equation[32] considering the following Hamiltonian:

$$\chi = \frac{N\mu_B{}^2}{4k_BT}\frac{g_{1/2}{}^2 + 10g_{3/2}{}^2\exp(3J/k_BT)}{1 + 2\exp(3J/k_BT)} \qquad (2)$$

where $g_{3/2} = (2g_{Ni} + g_V)/3$ and $g_{1/2} = (4g_{Ni} - g_V)/3$. The simulations of the experimental data using the above expression are quite satisfactory, as shown by the solid lines in Figure 4. The best sets of parameters obtained are $J = -8.9(1)$ cm^{-1}, $g_{Ni} = 2.18(2)$, and $g_V = 1.98(2)$ for **3** and $J = -10.0(1)$ cm^{-1}, $g_{Ni} = 2.12(2)$, and $g_V = 1.92(2)$ for **4**. The magnetic interactions between Ni^{II} and V^{IV} are therefore antiferromagnetic, which stablizes an $S = {}^1/_2$ ground state. This ground state is confirmed by the field dependence of the magnetization studied at 1.85 K, which is well reproduced by an $S = {}^1/_2$ Brillouin function (inset of Figure 4). Nag et al.[13] have recently reported exchange-coupled nickel(II)−vanadium(IV) complexes with weak ferromagnetic interaction ($J = +2-12$ cm^{-1}). Orthogonality of the magnetic orbitals of octahedral Ni^{II} ($d_{x^2-y^2}$ and d_{z^2}) and square-pyramidal V^{IV}═O (d_{xy}) centers is believed to be the reason for this ferromagnetic interaction.[37] As it appears from the molecular structures of **3** and **4**, the dihedral angle between the basal planes containing the Ni^{II} and V^{IV} centers is 58.27° (62.66° for **4**), which is sufficient to break the orthogonality of the magnetic orbitals, resulting in antiferromagnetic interaction in the present case. In fact, a number of heterodinuclear nickel(II)−copper(II) complexes have been reported in recent times[36,38,39] with closely similar antiferromagnetic behavior as reported for **3** and **4**.

Electronic Spectra. Electronic spectra of **3** and **4** have been recorded in dichloromethane, and the data are summarized in the Experimental Section. The features are quite similar for both compounds. A representative spectrum (compound **4**) is displayed in Figure S4 in the Supporting Information, which shows three d−d absorptions in the form of two broad bands and a shoulder appearing at 875 nm (ϵ, 75 mol^{-1} cm^2), 649 nm (45 mol^{-1} cm^2), and 503 nm. Corresponding band positions for **3** are at 857 nm (75 mol^{-1} cm^2), 631 nm (50 mol^{-1} cm^2), and 448 nm, respectively. In principle, several d−d absorptions are expected for Ni^{II} in an octahedral ligand field, and also for V^{IV} in a square-pyramidal environment.[40] Thus, for exchange-coupled heterodimetallic systems such as **3** and **4**, further discussions on the interpretation of their spectra may sound somewhat speculative because of the inherent complexities. All of the remaining bands appearing below 400 nm are due to ligand internal transitions.

Electrochemistry. The electrochemical behaviors of the dinuclear complexes **3** and **4** have been studied by cyclic voltammetry under nitrogen in acetonitrile solutions (0.1 M TBAP) using a platinum working electrode, in the potential range −2.0 to +2.0 V vs Ag/AgCl reference. Voltammetric features of **4** are displayed in Figure 5, showing a couple of electrochemical responses, one in the cathodic and the other in the anodic potential range. The observed redox potentials

(34) Liu, C. M.; Gao, S.; Hu, H. M.; Jin, X.; Kou, H. Z. *J. Chem. Soc., Dalton Trans.* **2002**, 598.
(35) Bencini, A.; Gatteschi, D. *EPR of Exchange Coupled System*; Springer-Verlag: Berlin, 1990.
(36) Gao, E.-Q.; Tang, J.-K.; Liao, D.-J.; Jiang, Z.-H., Yan, S.-P.; Wang, G.-L. *Inorg. Chem.* **2001**, *40*, 3134.
(37) de Loth, P.; Karafiloglou, P.; Daube, J. P.; Kahn, O. *J. Am. Chem. Soc.* **1988**, *110*, 5676.
(38) Terraco, J.; Diaz, C.; Ribas, J.; Ruiz, E.; Mahia, J.; Mestro, M. *Inorg. Chem.* **2002**, *41*, 6780.
(39) Gao, E.-Q.; Liao, D.-J.; Jiang, Z.-H.; Yan, S.-P. *Polyhedron* **2001**, *20*, 923.
(40) (a) Lever, A. B. P. *Inorganic Electronic Spectroscopy*, 2nd ed.; Elsevier Science BV: Amsterdam, The Netherlands, 1984. (b) Selbin, J. *Chem. Rev.* **1965**, *65*, 153.

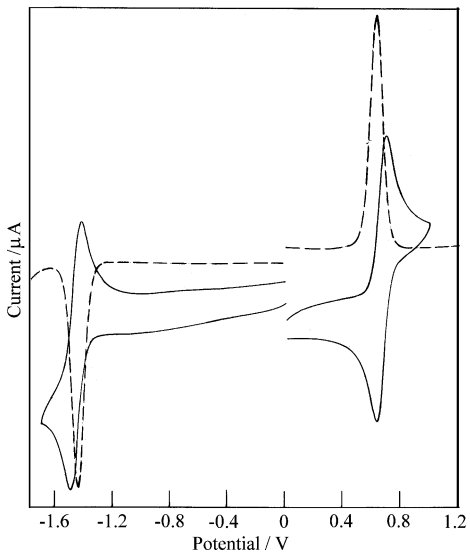

Figure 5. Cyclic voltammogram (—) of **4** in 0.1 M TBAP/acetonitrile at a platinum electrode (100 mV s^{-1}). For differential pulse voltammogram (− −): scan rate, 20 mV s^{-1}; pulse amplitude, 50 mV.

are $(E_{1/2})_1 = +0.66$ V (couple 1) and $(E_{1/2})_2 = -1.46$ V (couple 2). The ligands are electrode-inactive in this potential range. Both electron-transfer processes are reversible with the use of the criteria of the scan rate (50−500 mV s^{-1}) dependence of the peak current and width and equivalence of the cathodic and anodic peak heights.[41] The separation of the peak potentials (ΔE_p) is 59 mV for each couple. The electron stoichiometries for these couples were examined by constant-potential electrolysis with a platinum gauze working electrode. Exhaustive electrolysis past the oxidation process ($E_w = +0.90$ V) established a single-electron stoichiometry ($n = 1.0 \pm 0.08$ F mol^{-1}) for this couple. Similar experiments with the reduction process ($E_w = -1.7$ V), however, failed to provide any meaningful results because of constant coulomb counts. Nevertheless, the monoelectronic nature of the latter process has been established from the differential pulse voltammetric experiments that generated identical current heights for both of the couples, as displayed in Figure 5. The electrochemical results for **4** are thus consistent with two successive one-electron steps, as shown by eq 3 (L = β-diketonate).[42] We believe the reduction process here is more likely due to a nickel(II)−nickel(I) couple, which usually appears at a much more negative potential.[43,44]

$$[LNi^{I}L^{1}V^{IV}OL] \underset{(E_{1/2})_2}{\overset{+e^-}{\rightleftharpoons}} [LNi^{II}L^{1}V^{IV}OL] \underset{(E_{1/2})_1}{\overset{-e^-}{\rightleftharpoons}} [LNi^{II}L^{1}V^{V}OL] \quad (3)$$

Another alternative possibility is a V^{IV}/V^{III} reduction, which is expected to be followed by a chemical reaction involving $V{=}O_t$ bond cleavage. Such a process, unlike the present one, would give rise to an irreversible reduction. The latter process is, in fact, totally missing in the voltammogram of **3**, which displays a lone oxidation process at $(E_{1/2})_1 = 0.6$ V. This, we anticipate, is due to a $V^{IV}O/V^{V}O$ electron transfer. At this stage, we are not quite sure how a small change in the β-diketonate moiety can bring about such a prominent effect on the electrochemical behavior of **3**.

Concluding Remarks

Both tetra- and dinuclear heterometal complexes containing dinickel(II)−divanadium(V) and nickel(II)−vanadium(IV) metal-ion combinations, respectively, have been synthesized and structurally characterized by X-ray diffraction analysis. Fully deprotonated N_2O_2 ligand $(L^1)^{2-}$, capable of providing enough flexibility, binds the heterometal centers together through phenoxo bridging. The core structure in **1** and **2** is a centrosymmetric heterometallic eight-membered $Ni_2V_2O_4$ ring, unprecedented in the literature.[45] The magnetic measurements reveal that these tetranuclear complexes (**1** and **2**) may be regarded as magnetic dimers of octahedral Ni^{II} centers ($S = 1$) antiferromagnetically coupled (ca. $J = -3.7$ cm^{-1}) through diamagnetic $V^{V}O_2$ linkers. The metal centers in the dinuclear complexes **3** and **4** are also antiferromagnetically coupled (ca. $J = -9.5$ cm^{-1}), inducing an $S = {}^1/_2$ ground state. Both **3** and **4** are redox-active in a dichloromethane solution. While **4** undergoes a couple of reversible electron transfers involving a V^{IV}/V^{V} oxidation at $E_{1/2} = 0.66$ V and a Ni^{II}/Ni^{I} reduction at $E_{1/2} = -1.34$ V vs Ag/AgCl, the latter process is, however, missing in the voltammogram of **3**. It appears that an apparently innocent change in the β-diketonate structure has a significant influence in controlling the voltammetric features of the dinuclear complexes.

Acknowledgment. This work was partially supported by the Council of Scientific and Industrial Research (CSIR), New Delhi, India. Two of us (D.M. and P.B.C.) also thank the CSIR for the award of research fellowships. R.G. gratefully acknowledges the research grant received from the Department of Science and Technology, New Delhi, India, under SERC FAST Track Scheme. Financial support from the University of Bordeaux 1, from the CNRS, and from the French Ministries of Foreign Affairs and of Education and Research is gratefully acknowledged.

Supporting Information Available: X-ray crystallographic files in CIF format for compounds **1**−**4**, ESI-MS spectrum of **3**, ORTEP diagrams of **2** and **4**, and electronic absorption spectrum of **4** (Figures S1−S4). This material is available free of charge via the Internet at http://pubs.acs.org.

IC701925J

(41) Brown, E. R.; Large, R. F. In *Electrochemical Methods*; Weissberger, A., Rossiter, B., Eds.; Physical Methods in Chemistry; Wiley-Interscience: New York, 1971; Part IIA, Chapter VI.
(42) Net charge(s) on the complexes are omitted for clarity.
(43) Ghosh, D.; Mukhopadhyay, S.; Samanta, S.; Choi, K.-Y.; Endo, A.; Chaudhury, M. *Inorg. Chem.* **2003**, *42*, 7189.
(44) Bhattacharyya, S.; Weakley, T. J. R.; Chaudhury, M. *Inorg. Chem.* **1999**, *38*, 633.
(45) Allen, H. F. *Acta Crystallogr.* **2002**, *B58*, 380.